Effects of Aromatic Regularity on the Structure and Conductivity of Polyimide-Poly(ethylene glycol) Materials Doped with Ionic Liquid

Elyse Coletta,[1] Michael F. Toney,[2] Curtis W. Frank[1]

[1]Department of Chemical Engineering, Stanford University, Stanford, California 94305
[2]Stanford Synchrotron Radiation Lightsource, Menlo Park, California 94025
Correspondence to: E. Coletta (E-mail: elyse.coletta@gmail.com)

ABSTRACT: An understanding of the structure and properties of polymer electrolyte systems can be crucial to a variety of different applications. The current work performs a study of the composition, structure and properties of poly(ethylene glycol) (PEG)-aromatic polyimide systems incorporating ionic liquids that are relevant to several applications especially fuel cell membranes. Composition was varied through using different aromatic dianhydrides, aromatic diamines and in some cases synthesis solvent. Properties were characterized using Fourier transform infrared spectroscopy, thermal gravimetric analysis, differential scanning calorimetry, small-angle x-ray scattering, electrochemical impedance spectroscopy and cyclic voltamme-

try. By varying solvent, aromatic regularity and expected rigidity can be tuned, impacting average conductivity by 30%. Varying the aromatic diamine can influence the length scale and amount of aromatic regularity, which can ultimately affect the conductivity by a factor of four. The maximum conductivity reached was 83 mS/cm at 80 °C and 70 %RH. © 2015 Wiley Periodicals, Inc. J. Polym. Sci., Part B: Polym. Phys. **2015**, *53*, 509–521

KEYWORDS: copolymerization; membranes; poly(ethylene oxide); polyimides; SAXS; self-organization; structural characterization; structure-property relations

INTRODUCTION Polymer electrolyte systems are of great interest for a variety of applications including fuel cell membranes, battery electrolytes, actuators, gas separation membranes, and others.[1] It has been shown that the structure and properties of these systems are often linked but not always well understood. Furthermore, a substantial portion of previous studies has focused on well-ordered block copolymer systems to begin to link the nanometer level structure of such systems to their transport properties with far less attention being paid to random copolymer systems. Random copolymer systems can be more complex and potentially more ambiguous than block copolymer systems, but can show different properties than those in the well-ordered systems and are often simpler to synthesize. There has been some work done on understanding the properties of random copolymers, with the most relevant to the current work focusing on gas separation, dielectric characteristics, filtration, and in some select material cases conductivity.[2–10] These studies have begun to examine the relationship between structure and transport properties in random polymer materials, but more insight is still needed, especially with regard to linking electrolyte properties with a fundamental understanding of structure.

The primary goal of this material analysis is to examine the relationship between nanometer-scale structure and ionic conductivity, when the aromatic properties and interactions are varied in random copolymers of poly(ethylene glycol) PEG and aromatic polyimide (PI). In these random copolymers, the PEG domains primarily serve as the ion conducting phase and the aromatic polyimide serves as the mechanical matrix. We varied the supporting polyimide matrix to examine how polyimide regularity impacts structure and conductivity. The primary focus of this study was to gain some insight into the relationship between transport properties and structure of these polymer membranes and be able to link that information to a particular application of interest, proton exchange membrane fuel cells, as well as offering some conclusions that can be generalized to other applications including battery electrolytes, actuators, and filtration membranes.

Aromatic polyimides were an optimal polymer component choice because they possess excellent stability, more specifically thermal stability, chemical stability, and electrochemical stability.[11–14] Aromatic polyimides have great versatility

Additional Supporting Information may be found in the online version of this article.
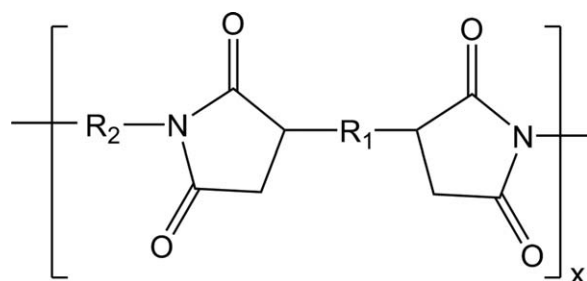
FIGURE 1 The general chemical structure of an aromatic polyimide reveals the versatility possible in the chemical structure.

because there are a wide variety of aromatic monomers that can be used in many combinations. Common aromatic polyimides have the general chemical structure seen in Figure 1. The R1 bridging group can contain various amounts of aromatic and non-aromatic character and can contain atoms including sulfur, fluorine, oxygen, and others. The R2 group can vary in aromatic character, size and functionality as well. Many different aromatic polyimides have been studied for various applications; in particular, the structural richness of this class of compounds has been studied in depth and is of most interest to the current work.

The R groups of polyimides often contain hexafluoro groups between two aromatic rings. Because of the bulky and relatively flexible nature of these hexafluoro bridging groups, the polymer chains tend not to have any regularity or order in their packing or positioning.[15–18] Some partially or nonfluorinated polyimides, where either R1 or R2 contain less bulky groups and have more aromatic character, have been shown to possess new structural features as compared with the fully fluorinated polyimides. These aromatic polyimides may show regular structural features on the order of 1 to 3 nm, which is roughly the size of the aromatic monomer or repeat unit. The more streamlined, less bulky aromatic portion of the polymer chain is more rigid and planar. The rigidity and planarity lead to a regularity in the orientation of the repeat unit of the polyimide that manifests as an ordered structural feature on the length scale of a few nanometers.[19–28] The rigidity and planarity of these less bulky aromatic rings give these polymers certain orientations and regularity that are not present in a flexible linear backbone polymer that is able to coil into a wider range of configurations.

The ability of less bulky aromatic polyimides to orient in specific ways on the length scale of a few nanometers can also extend to other length scales. Moreover, the ability of the more streamlined aromatic rings to share electrons through π-π stacking and other dipole-related interactions can result in a regular inter-chain spacing that can cause regularity on the sub-1-nanometer length scale. The presence of this short-range regularity predisposes the polymer to form ordered structures on longer length scales. The regions of polymer chains that have a very regular spacing, interaction and alignment form domains of dense, packed chains

similar to crystalline structures. This regularity can continue over a certain length scale until variation in the structure or defects in the material cause the regularity of the polymer chains to change. It has been hypothesized and modeled that there are then regions of very well-packed, crystal-like polymer chains along with regions of more amorphous, less regular polymer chains.[29–31] The domains of more-well-packed or less-well-packed polymer chains tend to alternate and form lamellar-like structures. The periodicities of these alternating regions typically are on the order of 10 nm and, thus, give rise to structural features on those length scales. Although short-length-scale order can be related to long-length-scale order, the longer scale order can also be present in these materials without the short-length-scale order.

The R groups in polyimides can also contain nonaromatic polymer components, such as PEG. Previous studies have been done on PEG-containing polyimides similar to those in the current work and provide insight into the structure and important parameters in these polymer systems, but more information on the interpretation of the SAXS results is needed to fully understand these types of materials.[5–8,32–40] Properties such as gas permeability and selectivity were also shown to depend on the polyimide bridging groups due to variations in free volume and the ability of the polymer chains to participate in close packing.[41,42]

Although several PEG-containing polyimides have been synthesized and characterized, very few of these studies have focused on assessing the ion transport properties and even fewer touch upon their relationship to polymer structure.[43] To our knowledge, the present work examines specific polyimides that have not been considered previously with emphasis on understanding the polymer physics associated with aromatic interactions and their relationship to structure and conductivity.

EXPERIMENTAL

Materials

4, 4′-(1,3-phenylenedioxy) dianiline (PDODA), 4, 4′-(hexafluoroisopropylidene) diphthalic anhydride (6FDA), poly(ethylene glycol) *bis*(3-aminopropyl) terminated (M_n 1500), 1-methyl-2-pyrrolidinone (NMP), and *N,N*-dimethylacetamide (DMAc) were purchased from Sigma Aldrich and used as received. 4, 4′-oxydiphthalic anhydride (ODPA) and 2, 2-*bis*(4-aminophenyl) hexafluoropropane (AP6F) were purchased from TCI America and used as received. Ethylammonium nitrate (EAN) was purchased from Iolitec and used as received. Teflon film was purchased from McMaster-Carr and used as received.

Synthesis

First, the *bis*(3-aminopropyl) terminated poly(ethylene glycol) and the aromatic diamine, either AP6F or PDODA, were placed into a three-neck flask. Then, the solvent, either DMAc or NMP, was placed into the flask. The contents were allowed to stir under nitrogen and gentle heating to approximately 50 °C

until all the solids were dissolved. The flask was then cooled to approximately 30 °C, and a stoichiometric amount of aromatic dianhydride, either 6FDA or ODPA, was added to the flask slowly and in solid form over a period of 30 min. The known total solids concentration was between 0.075 and 0.09 g/mL. The contents of the flask were allowed to stir at room temperature under nitrogen for 24 h and were then collected for future use as the PEG-containing poly(amic acid) precursor.

Casting/Imidization

The poly(amic acid) precursor solutions were poured into a Teflon-lined glass dish and thermally imidized in an oven using the following heating protocol: ramp from 20 °C to 90 °C over a period of 2 h and 15 min, then ramp to 130 °C over a period of 3 h, hold at 130 °C for 11 h, ramp to 155 °C over a period of 3 h, hold at 155 °C for 1 h, cool to 25 °C over a period of 4 h. The dry, free standing films were then collected for future testing.

Ionic Liquid Incorporation

The imidized free-standing films were cut into appropriate sizes and then placed into ethylammonium nitrate in a closed container at room temperature for 24 h and then removed immediately and tested as needed. Table 1 shows the key chemical structures of the polyimides synthesized, the ionic liquid and their corresponding abbreviations that will be used in subsequent discussions.

Characterization

Fourier transform-infrared spectroscopy (FT-IR) measurements were performed at room temperature using a Nicolet 6700 FT-IR. Sample preparation of the poly(amic acid) precursors involved drop casting a small amount of the poly(amic acid) solution onto a potassium bromide pellet and then subsequently removing the solvent by placing the pellet under vacuum at room temperature. Sample preparation for all fully aromatic polyimides and the dianhydride and diamine reactants involved crushing the samples into a powder and molding them into a potassium bromide pellet. The PEG-containing polyimides were dissolved in solvent and then drop cast onto a potassium bromide pellet. The solvent was subsequently removed by placing the pellet under vacuum at room temperature. FT-IR was used to qualitatively confirm the success of the undoped polymer synthesis.

Thermal gravimetric analysis (TGA) was performed using a Mettler Toledo TGA/SDTA 851e. Film samples between 1 and 15 mg were loaded into aluminum pans for testing. The thermal protocol involved heating from 25 °C to 600 °C at a rate of 10 °C per min. TGA was used to quantitatively determine the thermal stability of the undoped polymers in terms of mass loss as a function of temperature.

Differential scanning calorimetry (DSC) was performed using a TA Instruments Q100. Film samples between 1 and 10 mg were loaded into aluminum pans for testing. The following thermal protocol was used: equilibrate at 20 °C, ramp at 5 °C per minute up to 120 °C, hold at 120 °C for 2 min, ramp

at 5 °C per minute to 20 °C, hold at 20 °C for 2 min, then repeat the cycle two more times. DSC was used to qualitatively determine the undoped polymer morphology by detecting the presence or absence of calorimetric exotherms and endotherms.
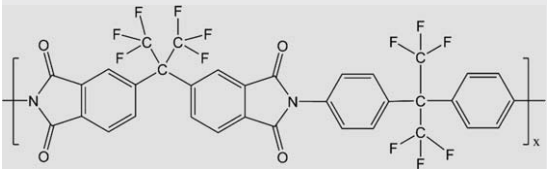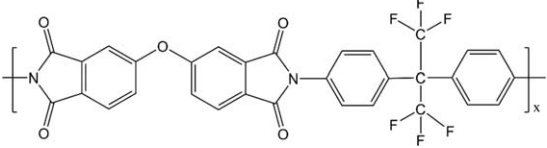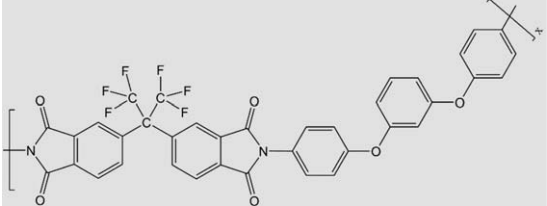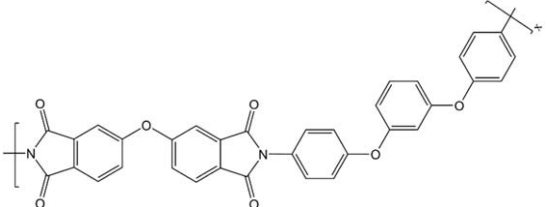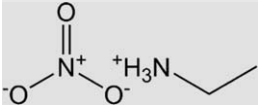
Ionic liquid uptake measurements were performed on a subset of the polymer materials. The undoped polymer was first weighed, then soaked in ethylammonium nitrate for 24 h at room temperature. The liquid-soaked polymer was then dabbed dry and reweighed to determine the amount of ionic liquid uptake. The reported values for the ionic liquid uptake are based on an average of three different measurements.

Conductivity measurements were performed using a BT 552 Bekktech conductivity analyzer and a Gamry Instruments Reference 600 Potentiostat/Galvanostat/ZRA via electrochemical impedance spectroscopy (EIS) and cyclic voltammetry (CV). The AC impedance was performed with an amplitude of 10 mV over a frequency range of 200,000 to 0.1 Hz, measuring 6 points per decade. Cyclic voltammetry was performed for five cycles over the voltage window of −0.1 to 0.1 V at a sweep rate of 25 mV/s with a step size of 2 mV and a maximum current range of 0.01 mA. Measurements were performed under nitrogen at 70% relative humidity between 40 °C and 80 °C, unless otherwise noted. An initial pretreatment at 60 °C for 45 min at low humidity was used in order to improve probe-to-film contact and have some equilibration of the equipment to the humidity levels. The conductivity values represent an average over three different films tested on different days with error bars representing one standard deviation above or below the average, unless otherwise noted. The individual film measurement values were based on an average of six measurements per single temperature on the same film. EIS and CV techniques were used to quantitatively assess the total and electrical conductivity, respectively, of the doped polymer films.

Small angle X-ray scattering (SAXS) was performed on beam line 1 to 4 at SLAC Synchrotron Radiation Laboratory (Stanford, CA). The wave length of the X-ray beam was 1.4884 Angstroms. Detector calibration was performed using silver behenate and chicken tendon. Data was averaged over space, and slit correction was used via Igor Nika software or a similar macro. All data are background corrected and based on an average exposure time of 5 min. All SAXS measurements were performed at room temperature and ambient humidity, unless otherwise specified. All ionic liquid-doped and elevated temperature membrane measurements were first pretreated at 60 °C for 45 min to mimic the pre-treatment performed before the conductivity measurements. Elevated temperature SAXS tests spanned a total duration of approximately 4 h.

Small-angle X-ray scattering qualitatively and quantitatively detected structural features on the length scale over a range between 0.5 and 80 nm. The exact sample analysis varied based on the specific material being considered. Various

TABLE 1 Chemical Structures of the Synthesized Polyimides and the Ionic Liquid with Their Corresponding Abbreviations

Chemical Structure	Abbreviation
	6FDA-AP6F
	ODPA-AP6F
	6FDA-PDODA
	ODPA-PDODA
	EAN

scattering models were used to extract phenomenological parameters. More information on these models and the assumptions that were used to evaluate the current materials can be found in the Supporting Information.

The parameters that can be deduced from the SAXS data with some certainty include the presence of phase separated domains, the spacing value of ordered domains, the approximate size of disordered domains and the relative amount of order for domains. Parameters that can be indirectly deduced from the data include relative domain connectivity. Parameters that cannot be determined from the data include, but are not limited to, the shape of domains, the location of domains, the size of ordered domains, the spacing value of any disordered domains and the amount of domain aggregation, phase separation, and domain ordering.

For the purposes of discussion, some of the key SAXS structural components are given code names with a P designation for peaks, S designation for shoulders, and F designation for more ambiguous features that either involve a very ill-defined peak with no clear maximum or a relatively narrow shoulder. A complete list of the features, their code names, and corresponding information are listed in Table 2. The

shoulders typically represent randomly distributed PEG domains across all polyimide families and occur at relatively similar length scales across materials. The peaks can correspond to aromatic polyimide ordering and/or ionic liquid doped-PEG ordering depending on the specific material. The less well-defined features correspond to aromatic polyimide order that has been impacted in some way by PEG and or ionic liquid. The key features will be discussed in more detail in subsequent sections.

RESULTS AND DISCUSSION

Synthesis of Undoped Polymers and Precursor Solutions
FT-IR was performed on the poly(amic acid) precursors and the final polymers in order to verify the success of the synthesis. The FT-IR spectra of the polyimides include peaks consistent with imidization around 1720 and 1780 cm^{-1}, which correspond to symmetric and asymmetric stretching of the carbonyl groups in the polyimide, respectively.[44–46] There was also a reduction or in some cases almost complete disappearance of the features in the range between 1400 and 1675 cm^{-1}, which corresponds to C=O stretching and CONH vibration of the poly(amic acid).[46,47] Through

TABLE 2 List of Materials, Key SAXS Structural Components, and Associated Information

Material	Feature Code	Feature Origin	ξ or d Value (nm)	q Value (nm^{-1})
ODPA-PDODA	P_{ahOO}	Average inter-chain spacing	0.5	12.6
	P_{asrOO}	Aromatic polyimide order (aromatic repeat unit)	2.4	2.6
	P_{alrOO}	Aromatic polyimide order (longer range order)	11.7	0.54
6FDA-PDODA	P_{ahFO}	Average inter-chain spacing	0.5	12.6
	P_{aFO}	Aromatic polyimide order (aromatic diamine repeat unit)	1.9	3.4
ODPA-AP6F	P_{ahOF}	Average inter-chain spacing	0.6	10.5
6FDA-AP6F	P_{ahFF}	Average inter-chain spacing	0.6	10.5
ODPA-PDODA-ODPA-PEG1500	P_{ashOO}	Aromatic polyimide order (aromatic repeat unit)	2.3–2.5	2.7–2.5
	F_{lrOO}	Aromatic polyimide order with PEG interference	13.7–19.6	0.48–0.32
ODPA-AP6F-ODPA-PEG1500	S_{PEGOF}	Disordered PEG domains	0.7[a]	∼2
	P_{aOF}	Aromatic polyimide order (aromatic dianhydride repeat unit)	14.5–15.3	0.43–0.41
ODPA-AP6F-ODPA-PEG1500 (50%) DMAc	S_{PEGOF}	Disordered PEG domains	0.9	∼2
	P_{aOF}	Aromatic polyimide order (aromatic dianhydride repeat unit)	15.3	0.41
ODPA-AP6F-ODPA-PEG1500 (50%) NMP	S_{PEGOF}	Disordered PEG domains	0.6	∼2
6FDA-PDODA-6FDA-PEG1500	S_{PEGFO}	Disordered PEG domains	0.4[a]	∼2
	F_{aFO}	Aromatic polyimide order with PEG interference	1.9–2.6	3.3–2.4
6FDA-AP6F–6FDA-PEG1500	S_{PEGFF}	Disordered PEG domains	0.6[a]	∼2
ODPA-AP6F-ODPA-PEG1500 (50%) EAN NMP	$P_{PEGILOF}$	IL-doped PEG order (spacing of doped PEG domains)	15.0	0.42
ODPA-AP6F-ODPA-PEG1500 (50%) EAN DMAc	F_{aOF}	Aromatic polyimide order with IL interference	15.0[b]	0.42
	$P_{PEGILOF}$	IL-doped PEG order (spacing of doped PEG domains)	11.6	0.54
ODPA-PDODA-ODPA-PEG1500 (50%) EAN	P_{asrOO}	Aromatic polyimide order (aromatic repeat unit)	2.6	2.4
	F_{lrOO}	Aromatic polyimide order with PEG and IL interference	25.1[b]	0.25

d value corresponds to peaks and features. ξ value corresponds to shoulders.

[a] Indicates average over material composition space.
[b] Indicates estimated spacing from a less-well-defined feature.

both the appearance of new features and the disappearance or loss of prominence of other features, FT-IR confirmed that the initial synthesis resulted in poly(amic acid) and that the final membranes were polyimides based on absorption bands seen in polyimides from previous work.

Thermal Stability of Undoped Polymers
As a first step in evaluating the properties of the PEG-containing polyimides, TGA was performed on the polymers to assess their ability to function in a moderate temperature

fuel cell environment. The thermal stability results for all of the aromatic polyimide families were largely similar, and representative results for the 6FDA-AP6F family can be seen in Figure 2.

The PEG 1500 diamine reactant is presented for reference and shows essentially complete mass loss starting at a temperature around 300 °C and ending by around 400 °C. The mass loss before 400 °C seen in the fully aromatic polyimide, 0 wt % PEG, and in the 10 wt % PEG-containing polyimide
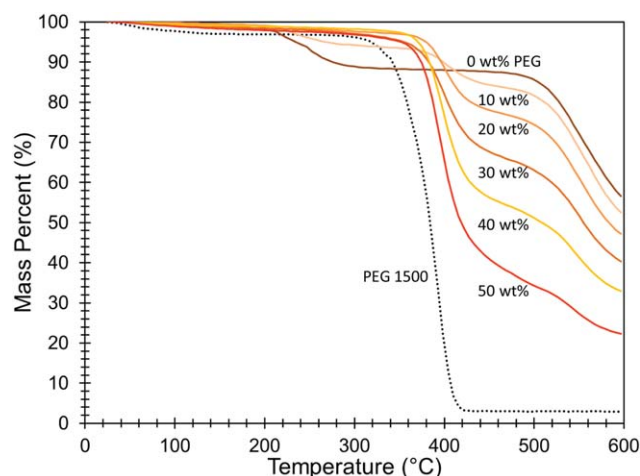
FIGURE 2 TGA curves of the 6FDA-AP6F family of PEG-containing polyimides with varying PEG weight percent. [Color figure can be viewed in the online issue, which is available at wileyonlinelibrary.com.]

is believed to be evidence of incomplete imidization and corresponds to degradation of the poly(amic acid) that has not been completely imidized into the polyimide ring structure. The TGA data shows a significant mass loss at 400 °C in all of the PEG-containing compounds, which is most likely due to the degradation of the PEG component of the PEG-containing polyimides, with the mass loss increasing as the amount of PEG incorporated in the polymer increases. The significant mass loss around 400 °C that is attributed to PEG degradation occurs at a temperature similar to mass losses around 250 to 450 °C that were attributed to the PEG component in similar PEG-containing copolymers in previous work.[5–8,32,33] The significant mass loss at 550 °C occurs across all of the materials and is likely due to the degradation of the polyimide component. The mass loss decreases as the amount of aromatic polyimide decreases in the polymers. This mass loss occurring around 550 °C, attributed to the polyimide phase degradation, occurs at a similar temperature to mass losses assigned to the aromatic polyimide component in PEG-containing copolymers in previous work at around 450 °C and higher.[5–8,32,33]

The thermal stability of the polymers was found to be sufficient for the fuel cell application operating conditions. There is less than 5% mass loss of the compounds for temperatures up to around 200 °C, which yields a more-than-adequate expected operating window for the fuel cell. The thermal stability of the materials is primarily dominated by the amount of PEG incorporated into the polyimide, with an increase in stability corresponding to a decrease in PEG content. Lower temperature mass losses for the lowest PEG content film and the fully aromatic polyimide are attributed to regions of incompletely imidized polymer chains possibly resulting from less chain flexibility. With increasing PEG content, the flexibility of the polymer chains increases, which can lower the barrier to chain motion required for imidization.[9,14] As a result, the higher PEG content materials would

be expected to have more complete imidization and in fact do not show any lower temperature mass loss.

Morphology of the Undoped Polymers

The morphology of the undoped polymers is also important to understand with regard to conductivity. Similarly to the thermal stability results, the morphological results were comparable across all families of aromatic polyimides, and the DSC results for the 6FDA-AP6F family are presented in Figure 3 as a representative data sample. The second heating cycle data shows that the PEG diamine exhibits a melting endotherm at around 48 °C. Once the PEG is incorporated into the aromatic polyimides (weight fractions ranging from 10 to 50%) and processed, there is no evidence of PEG crystallinity.

If the polycondensation reaction proceeds as expected, the PEG chains are surrounded on each side by an aromatic monomer and are thus likely to be relatively isolated. The PEG is also expected to segregate away from the polyimide based on evidence of phase separation in previously studied PEG-containing polyimides.[5] However, such phase separation will be controlled by the covalent bonds between PEG and PI, much like block copolymers. For relatively short PEG segments, the mobility and configuration will be constrained by the surrounding material, thus retarding PEG crystallization.

Moreover, similar PEG-containing polyimides with certain processing conditions have also shown no evidence of PEG crystallinity.[7,36,48–50] Amorphous PEG morphology is advantageous for higher conductivity because the less tightly associated chains can associate with and transport ions in an easier fashion.[51,52] The amorphous morphology over the tested temperature material range persists in spite of variation in amount of PEG and changes in polyimide family.

Structure of Undoped Polymers

The structures of the undoped polymers were examined in-depth through systematic material variation. The family of materials analyzed was chosen to help elucidate the various structural features in these polymer systems and aid in interpretation. This information is in support of the main findings and detailed discussion can be found in the Supporting Information.

To summarize the analysis of the structure of the undoped polymers, these copolymers show varying levels of structural richness on different length scales at the nanometer level. SAXS revealed changes in the nanometer-scale structure of these compounds with changes to the aromatic monomers and the PEG weight percent. Good control over PEG domain size, on the order of 1 to 4 nm when size could be determined, and film formation behavior was achieved over a wide range of PEG content, from 0 to 50 wt %. Thus, free standing films with good structural control were obtained.

The ODPA-PDODA family showed both short and long range aromatic regularity that become less pronounced with the addition of PEG. The ODPA-AP6F family showed evidence of long range aromatic regularity, apparent only at higher PEG
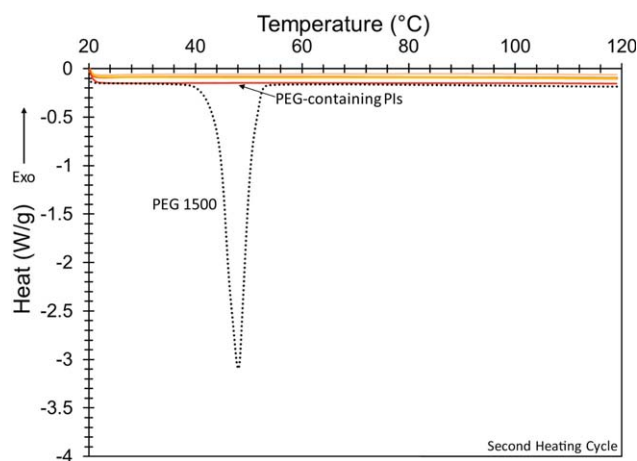
FIGURE 3 DSC curves of the 6FDA-AP6F family of PEG-containing polyimides with PEG weight percent ranging from 10 to 50 percent. [Color figure can be viewed in the online issue, which is available at wileyonlinelibrary.com.]

weight contents, which could be tuned through variations in processing. Short range aromatic regularity that lost prominence as PEG was introduced into the material was observed for the 6FDA-PDODA family. Finally, no aromatic regularity was observed in the 6FDA-AP6F family.

Overall, the ODPA-AP6F family has the largest average PEG domains followed by the 6FDA-AP6F family with the smallest PEG domains occurring for the 6FDA-PDODA family. The size of the PEG domains in the ODPA-PDODA family could not be determined. The ODPA-AP6F family may have the largest PEG domains due to larger or more extended domains being favorable for aromatic phase ordering. The 6FDA-AP6F family has relatively large free volume from bulky monomers and so relatively large PEG domains may be expected for this polyimide family. In addition, miscibility differences or short range aromatic order steric interference may explain the smallest PEG domains in the 6FDA-PDODA family. The variety of structural features achieved from these different polyimide families make this class of materials an interesting set to examine for further structure-property insights.

Structure, Ionic Liquid Uptake, and Conductivity of Polymers

By understanding not only composition and structure, but also conductivity, the link between aromatic ordering and properties can be determined. Initial evidence has shown that changes in material composition and processing lead to changes in material structure and the hypothesis is that those structural changes will correspond to changes in conductivity. Although a large suite of polymers was chosen for structural study only a small subset were chosen for the structure-property relationship analysis. The material variations chosen for the structure-property analysis were based on the specific hypothesis that the conductivity of a polymer with a flexible matrix will be greater than the conductivity of a polymer with a rigid matrix. Since previous studies on polyimides have sug-

gested links between structural order and rigidity, those polymers with variable aromatic order were chosen to be the focus of the structure-property analyses in order to achieve polymers with matrices of variable rigidity.[53,54]

ODPA-AP6F Family: Impact of Changing Solvent

The ODPA-AP6F family of PEG-containing polyimides showed evidence of aromatic regularity, thus, this particular polymer family was of special interest. The 50% PEG material was chosen for primary focus since that material possessed the most pronounced aromatic structure. Initial evidence also suggested that the polymer structure of ODPA-AP6F-ODPA-PEG1500 (50%) can be varied by changes in processing conditions and as such, the synthesis solvent for this polymer was varied in order to systematically asses any changes in structure and subsequent changes in transport properties. The solvents used for the synthesis were either DMAc or NMP. The structures of the polymers synthesized in these two solvents can be seen in Figure 4. The shoulder attributed to the randomly distributed PEG domains, S_{PEGOF}, showed some minor changes with solvent variation. In contrast, the peak attributed to aromatic ordering of the ODPA units, P_{aOF}, showed major changes when the solvent was varied. More specifically, the SAXS shows that both materials have a shoulder, S_{PEGOF}, of similar correlation length, 0.9 nm for the DMAc-synthesized system and 0.6 nm for the NMP-synthesized system. The different correlation lengths correspond to estimates of two PEG chains per domain for the DMAc-synthesized polymer as opposed to 1.3 PEG chains per domain for the NMP-synthesized polymer. If the correlation lengths are converted to radii, there is a PEG domain radius of 1.0 nm for the NMP-synthesized system and 1.6 nm for the DMAc-synthesized system. Additionally, the material synthesized in NMP shows no evidence of P_{aOF}, but in the DMAc-synthesized material P_{aOF} has a spacing value of 15.3 nm ($q = 0.41$ nm^{-1}).
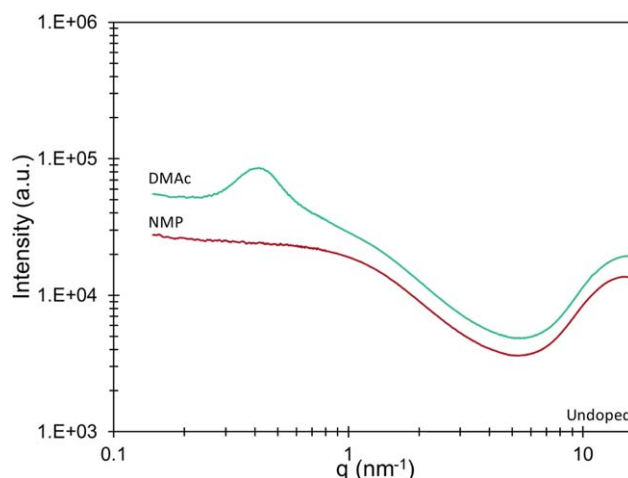

FIGURE 4 SAXS signatures of the ODPA-AP6F-ODPA-PEG1500 (50%) polymer synthesized in DMAC and NMP. [Color figure can be viewed in the online issue, which is available at wileyonlinelibrary.com.]
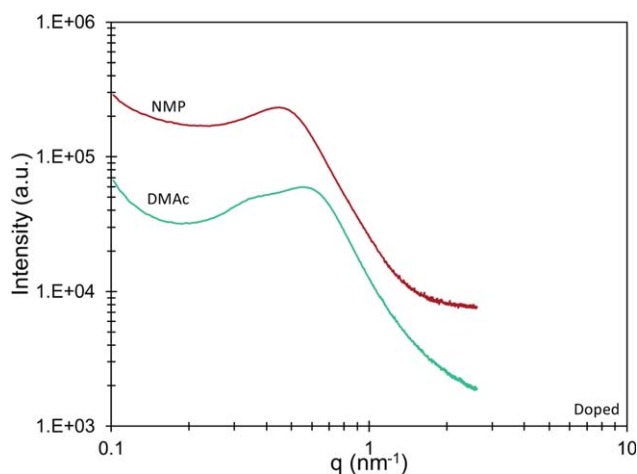
FIGURE 5 SAXS signatures of the ODPA-AP6F-ODPA-PEG1500 (50%) EAN material synthesized in DMAC and NMP. [Color figure can be viewed in the online issue, which is available at wileyonlinelibrary.com.]

The lack of P_{aOF} with the use of NMP is likely due to residual solvent effects. The more aromatic nature of the NMP solvent makes it less volatile and more miscible with the aromatic polyimide. If the peak results from aromatic ring interaction, the presence of solvent may cause more aromatic ring-solvent interactions instead of ring-ring interactions; thus, any peak resulting from the regularity in ring-ring interactions would be impacted. If the peak is due to alignment, the presence of solvent may impact the polyimide's ability to align since the solvent has no preferred direction and may cause polyimide swelling.

Also, the smaller PEG domains in the NMP-synthesized system may be due to the strongly hydrophobic nature of the solvent driving the PEG to segregate away from the solvent and the slightly more swollen aromatic polyimide. The smaller domains could also be a result of less extended polymer chains or less aggregated polymer chains due to the lack of P_{aOF} formation. The fact that changes to the peak occur upon solvent changes supports this feature indeed being related to the aromatic phase of the material.

The change in solvent produces one system with P_{aOF}, DMAc, and one without, NMP. The polymer synthesized in DMAc is expected to have more rigidity than that synthesized in NMP because of the presence of the polyimide order. This expectation is based on previous studies of aromatic polyimides sug-

TABLE 3 Ionic Liquid Uptake Values of ODPA-AP6F-ODPA-PEG1500 (50%) EAN Material Synthesized in DMAC and NMP

Material	Ionic Liquid	Uptake (%)
ODPA-AP6F-ODPA-PEG1500 (50%) DMAc	EAN	149
ODPA-AP6F-ODPA-PEG1500 (50%) NMP	EAN	184

gesting that interactions and structural order generally increase rigidity.[53–55]

The structures of the EAN-doped polymer structures were also compared, as is seen in Figure 5. The DMAc-synthesized polymer shows a weak shoulder-like feature, F_{aOF}, at an estimated spacing value of 15.0 nm ($q = 0.42$ nm^{-1}), which is likely the remnants of P_{aOF} from the undoped polymer. P_{aOF} in the DMAc-synthesized material is transformed into F_{aOF}. This system also shows a peak that is related to the ionic liquid incorporation with a spacing value of 11.6 nm ($q = 0.54$ nm^{-1}), $P_{PEGILOF}$. The NMP-synthesized material only shows a broad maximum related to the ionic liquid incorporation, $P_{PEGILOF}$, at a spacing value of 15.0 nm ($q = 0.42$ nm^{-1}).

Based on previous studies done on PS-b-PEO systems, an ionic liquid is much more likely to associate with the PEG portion of the polymer; thus, the new structural feature seen likely represents the spacing between IL-doped PEG domains.[1,56–59] Block copolymers in general can undergo major structural changes upon being swollen with ionic liquid with one such transition involving the disordered state changing to an ordered state, which is analogous to the current material. The PEG domains, through swelling, seem to have become more ordered than in the undoped polymer case where they were disordered.

The structures of the EAN-doped polymers were also evaluated at elevated temperatures. There were no significant changes to note in the DMAc-synthesized material. On the other hand, the NMP-synthesized material did show significant changes. $P_{PEGILOF}$ has a spacing value that increases from 12.6 to 16.5 nm as the temperature increases, which is a large shift. The spacing value increases smoothly with temperature with small increases at low temperatures and then larger increases at higher temperatures, especially at 70 °C. The relative definition of the peak decreases significantly at temperatures above 60 °C. The extent of thermal changes that occur in this material due to thermal motion suggest a significant amount of material swelling and possible loss or leakage of ionic liquid especially at 70 and 80 °C where the structural peak loses definition. The large increase in the spacing value in the NMP-synthesized material could be due to chain swelling that is magnified by the lack of rigid polyimide ordering. This excessive swelling could then cause a loss of ionic liquid.

In order to compare these materials further, the ionic liquid uptake values were recorded and evaluated with the results seen in Table 3. The uptake values reveal that the NMP-synthesized material absorbs more ionic liquid than the DMAc-synthesized material, although the ionic liquid uptake values are both on the same order of magnitude.

The NMP-synthesized system is expected to be have less rigidity because there is no P_{aOF}, although the differences between the two materials synthesized in different solvents are somewhat minimal as the aromatic structural element
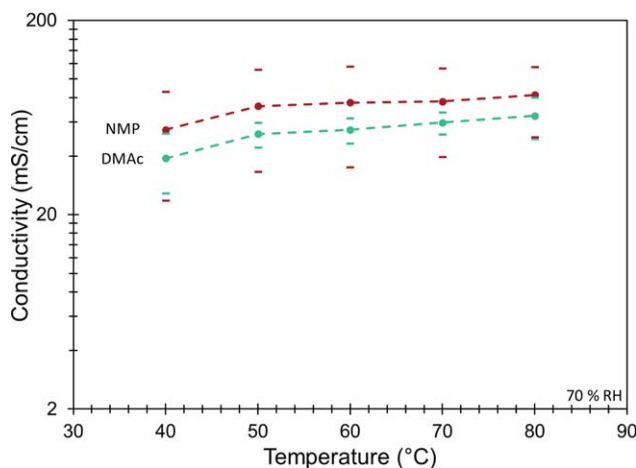
FIGURE 6 Conductivity of the ODPA-AP6F-ODPA-PEG1500 (50%) EAN material synthesized in DMAC and NMP at 70 % RH. [Color figure can be viewed in the online issue, which is available at wileyonlinelibrary.com.]

loses prominence and becomes F_{aOF} once the polymers are doped. The lack of aromatic rigidity in the NMP-synthesized system could make ionic liquid uptake easier explaining the higher amount of ionic liquid in that system. Also, there is expected to be more residual solvent in the NMP-synthesized polymer, which could leave more free volume in the polymer for ionic liquid during the doping process. These two factors may explain the higher ionic liquid uptake measured. An increase in free volume and decrease in rigidity are also expected to generally give more polymer chain mobility for possible transport.

The conductivity of these two materials at 70% RH synthesized in different solvents is compared in Figure 6. The conductivity generally increases as temperature increases for both polymer systems, as expected from diffusion behavior with estimated activation energies on the order of 8 to 11 kJ/mole.[60] These activation energy values are in relatively good agreement with those found for PEG-poly(methacrylate) systems doped with acetic acid, which ranged from 5 to 30 kJ/mole.[61] On average, the conductivity of the NMP-synthesized material is 30% higher than that of the DMAc-synthesized material. However, the conductivity variation of the NMP-synthesized material is very large.

The average conductivity correlates with the ionic liquid uptake, free volume, and rigidity trends expected in the materials. This trend mimics those of other transport property trends seen in other polyimides whereby more free volume and less rigidity generally correlate with an increase in transport.[41,42,53,54] The NMP-synthesized material has higher ionic liquid uptake and less expected rigidity from the lack of aromatic interactions or alignment. The higher ionic liquid uptake allows for more ions and the lack of the rigid aromatic polyimide structural component will allow more polymer chain mobility, and thus, ion mobility.

Although the NMP-synthesized film does perform better on average, its variation in performance is very large and spans a range that encompasses and exceeds the entire range of variation for the DMAc-synthesized film. This large amount of variation could be from a larger variation in the material synthesis with NMP as opposed to DMAc or reactivity differences. The variation could also be due to material swelling, as was suggested by the elevated temperature structural peak shift, because there are no regions of well-ordered polyimide lending structural stability. The material swelling could also be accompanied by ionic liquid loss, which is also expected to impact conductivity significantly.

The change of solvent impacts the presence of aromatic ordering on the length scale of around 15 nm, which in turn impacts the structure of the aromatic phase. The rigidity and free volume associated with the presence or absence of aromatic regularity ultimately influences the ionic liquid content and conductivity. These changes are moderately significant, impacting average conductivity by 30%.

ODPA Family: Impact of Changing Aromatic Diamine

It has been shown in the previous section that variation of the synthesis solvent can change the aromatic ordering in the polyimide phase which can lead to changes in conductivity. Another method of changing the nature of the aromatic ordering, as seen in the discussion of the undoped polymer structures, is to change the aromatic diamine. In the current material analysis, the impact of changing the aromatic diamine when using ODPA as the dianhydride will be examined.

The structural features of the undoped polymers with different aromatic diamines, as evidence by SAXS, can be seen in Figure 7. These two polymer systems show dramatic structural differences when the aromatic diamine is changed, with variations to both the type and length scale of features observed. The phase separation of the PEG from the polyimide is clear in the AP6F family with the presence of the shoulder attributed to PEG domains, S_{PEGOF}. There is also a peak attributed to aromatic interaction or alignment, P_{aOF}, at a length scale of around 15 nm which is expected to impart some rigidity to the material. These PEG and aromatic features are similar to others found in PEG and imide segment systems studied previously.[37,40,62–65]

The PEG phase is less well understood in the PDODA case due to the structural dominance of the polyimide structural characteristics P_{asrOO} and F_{lrOO}. These features arise from polyimide interaction or alignment on short and long length scales, and are comparable to aromatic features in other aromatic polyimides.[55,66–68] The features related to polyimide regularity may be overshadowing any feature corresponding to the PEG on the nanometer scale. Alternatively, the rigid ring interactions or preferred orientations could be preventing or altering the small-scale interaction of PEG with the polyimide due to steric interference. Yet another explanation of the structural features seen is that the PEG phase separation could be less well-defined due to increased phase miscibility.
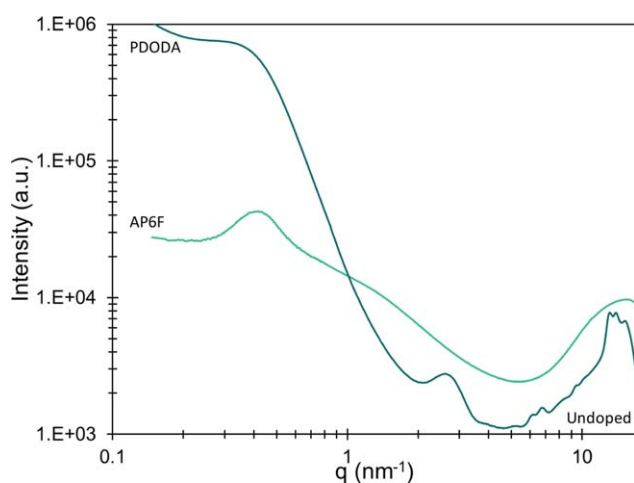
FIGURE 7 SAXS signatures of ODPA-AP6F-ODPA-PEG1500 (50%) and ODPA-PDODA-ODPA-PEG1500 (50%) materials. [Color figure can be viewed in the online issue, which is available at wileyonlinelibrary.com.]

Regardless of the exact nature of the PEG domains, the PDODA material is expected to be more rigid due to the regions of interacting or aligned rings on both short and long length scales, on the order of 2 to 3 nm and 19 to 20 nm. Ordering on a shorter length scale, as evidence from the short range feature P_{asrOO}, is expected to lead to more rigidity on the molecular level since the length scale of the order is approaching the molecular length scale. Increases in rigidity have been seen and modeled in similar polyimides with ring interactions and alignment that produce ordered structural features.[53–55,66–68] In addition to changes in structure between polymers, there are some noticeable changes in polymer structure when comparing the undoped and doped polymer systems.

The SAXS signatures of the ionic liquid doped polymers can be seen in Figure 8. To briefly reiterate the AP6F family case seen in the previous section, the polymer has undergone significant structural changes as compared with the undoped polymer. F_{aOF}, related to the once prominent aromatic feature, P_{aOF}, has an estimated spacing value of 15.0 nm ($q = 0.42$ nm^{-1}) and $P_{PEGILOF}$ related to the ionic liquid-doped phase has a spacing value of 11.6 nm ($q = 0.54$ nm^{-1}). Overall, the structure of the PDODA family does not change as significantly upon doping. The PDODA family case shows a broad ill-defined shoulder at longer length scales, F_{lrOO}. This element is possibly a convolution of a possible weakly defined feature related to the ionic liquid-doped PEG phase and the disordered or diluted F_{lrOO} seen previously in the undoped polymer. The spacing value of F_{lrOO} can be estimated to be 25.1 nm ($q = 0.25$ nm^{-1}), which is a larger value than in the undoped polymer, indicating some effect on this feature from the ionic liquid. There is also the presence of the maximum, P_{asrOO}, at a spacing value of 2.6 nm ($q = 2.4$ nm^{-1}). Although P_{asrOO} has been weakened slightly

in definition from the presence of PEG and ionic liquid, its position has not shifted significantly.

The AP6F system shows changes in structure upon doping with the transformation of P_{aOF} into F_{aOF}, and the transformation of S_{PEGOF} into $P_{PEGILOF}$ likely from rearrangement and ordering. The PDODA structure, on the other hand, did not change dramatically from the undoped polymer structure. Definition of the polyimide features, both P_{asrOO} and F_{lrOO}, was somewhat weakened due to the presence of ionic liquid. Also, F_{lrOO} shifted to a somewhat larger spacing value likely due to some amount of chain swelling or reorganization. Although some structural changes occurred in the PDODA material, the changes were not as dramatic as the AP6F material. In both systems, the presence of some structural change upon doping is analogous to structural rearrangement with the addition of ionic liquid to block copolymer systems seen previously in other studies.[56–59] A key structural trend is that the dominant order is present in the ionic liquid-doped PEG phase for the AP6F material and the dominant order in the PDODA material is in the aromatic phase. The order of the ionic liquid-doped PEG phase suggests more directed ionic conduction pathways through the material. The dominant aromatic order suggests rigidity in the polymer. The ionic liquid-doped polymer structures were also examined at elevated temperatures but showed no major changes, suggesting that there was no significant loss or leakage of ionic liquid.

To compare the materials further, the ionic liquid uptake was measured with the results shown in Table 4. The ionic liquid uptake is quite significantly lower for the PDODA system compared with the AP6F system. The ionic liquid uptake values somewhat correlate with the type and amount of structural changes to the polymers once doped.
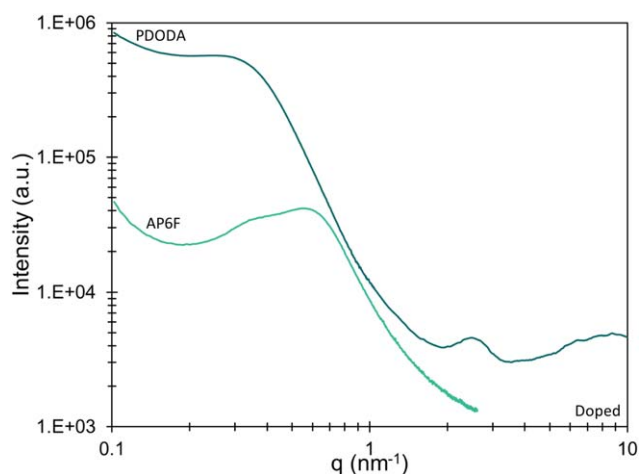

FIGURE 8 SAXS signatures of ODPA-AP6F-ODPA-PEG1500 (50%) EAN and ODPA-PDODA-ODPA-PEG1500 (50%) EAN materials. [Color figure can be viewed in the online issue, which is available at wileyonlinelibrary.com.]

TABLE 4 Ionic Liquid Uptake Values of ODPA-AP6F-ODPA-PEG1500 (50%) EAN and ODPA-PDODA-ODPA-PEG1500 (50%) EAN Materials

Material	Ionic Liquid	Uptake (%)
ODPA-AP6F-ODPA-PEG1500 (50%)	EAN	149
ODPA-PDODA-ODPA-PEG1500 (50%)	EAN	65

In the PDODA system, there is probably more rigidity imparted to the polymer chains from the presence of the short and long range polyimide structural features, P_{asrOO} and F_{lrOO}. This rigidity would impede the mobility of the polymer, likely both the PEG and PI phases, and cause a tendency for less reorganization, less swelling and less ionic liquid uptake, which is supported by the doped structural data and the ionic liquid uptake data. Trends showing that rigidity reduces the polymer mobility have been seen in similar previously studied polyimides.[41,42,54] There is also no clear presence of any structural features related to the ionic liquid in the PDODA material. This lack of a defined feature related to the ionic liquid correlates with less liquid uptake, which will mean less ions and less reorganization into well-directed ionic liquid-doped PEG domains. Less well-defined conductive domain alignment means more tortuosity and randomness of the pathways, and in modeled block copolymer materials also correlates with a decrease in transport and conductivity.[56–59]

It is also possible that any potential feature related to the ionic liquid is less well-defined due to larger scale or less defined PEG phase separation. If the phase separation of the PEG in the PDODA case is not as well-defined, there will be even more rigidity imparted to the PEG than if the phases were more distinct. It is also possible that the PEG is not interacting in the same manner on the nanometer-scale with the polyimide phase in the PDODA material due to interfer-

FIGURE 9 Conductivity of ODPA-AP6F-ODPA-PEG1500 (50%) EAN and ODPA-PDODA-ODPA-PEG1500 (50%) EAN materials at 70 % RH. [Color figure can be viewed in the online issue, which is available at wileyonlinelibrary.com.]

ence from the polyimide structural features. This type of behavior could also decrease the conductivity if the PEG domains are ill-defined.

The fluorinated diamine is expected to provide more free volume than the ether-containing diamine based on size and previous studies done on polyimides with various monomer types including ether linkages, methyl group linkages, adjacent aromatic rings and different substituted aromatic rings.[53,54] An increase in free volume is likely to lead to a higher ionic liquid uptake and, thus, a higher ion population as well as more space for the polymer chains to move. The fluorinated diamine also prevents very regular interaction and alignment of the aromatic rings. P_{aOF}, which likely only involves the ether-containing dianhydride, will not provide as much rigidity as the short range and long range features, P_{asrOO} and F_{lrOO}, which likely involve the entire aromatic repeat unit in the PDODA material. The amount of ionic liquid uptake will be due to the balance of the swelling forces with the rigidity of the polyimide. The aromatic polyimide rigidity as well as the relative definition and ordering of the ionic liquid-doped domains are related and are expected to impact transport.

Figure 9 shows the conductivity results upon changing the aromatic diamine within the ODPA family. As expected based on diffusion behavior, the average conductivity generally increases with an increase in temperature for both polymers, with estimated activation energies on the order of 5 to 11 kJ/mole, which are in relatively good agreement with those of PEG-poly(methacrylate) systems doped with acetic acid ranging from 5 to 30 kJ/mole.[60,61] More dramatically, there is a significant decrease in the conductivity, by a factor of 4, when going from the fluorinated diamine to the ether-containing diamine. The conductivity results correlate with the rigidity expected for the polymers. In particular, the results are consistent with similar trends showing a decrease in transport for an increase in rigidity in other polyimides.[41,42,53,54]

This rigidity will not only impact the ability of the polymer chains to move and transport ions but will also impact the amount of ionic liquid uptake. The amount of ionic liquid uptake will in turn impact the ion concentration and the definition and direction of the doped pathways through the material as is seen in the structural differences. Less ions, more disordered, ill-defined pathways and more rigidity all contribute to the lower conductivity for the PDODA material. The identity of the aromatic diamine in this case affects the amount and length scale of the aromatic order which ultimately has a profound influence on the structure and performance, changing conductivity by a factor of 4.

CONCLUSIONS

The data presented suggests that the thermal stability of PEG-containing polyimides is sufficient for the intended fuel cell applications and is relatively independent of choice of aromatic polyimide. The morphology of the undoped
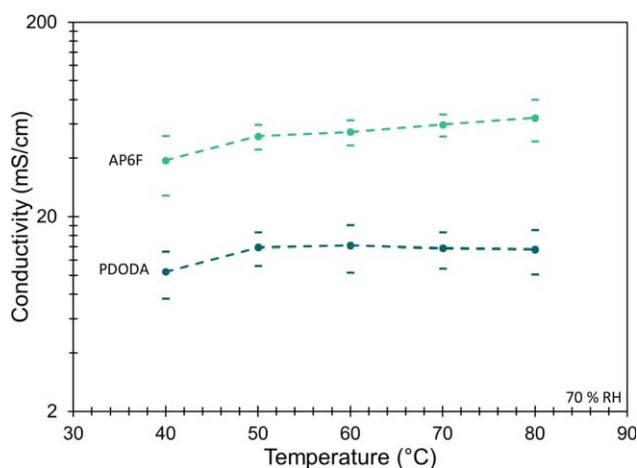
polymers was also tested and was found to be amorphous and independent of PEG weight percent and choice of aromatic polyimide. The structures of the undoped polymers were then analyzed and found to vary depending on the exact choice of aromatic dianhydride and diamine and in some cases processing. The amount of aromatic ordering as well as the length scale of ordering could be tuned by changing the choice of aromatic dianhydride, aromatic diamine, and solvent. The various types of aromatic ordering are expected to impact the polymer rigidity and free volume.

Changing the synthesis solvent in the ODPA-AP6F family can impact the aromatic structural order, which can lead to differences in rigidity, free volume, ionic liquid uptake and ultimately average conductivity. Similar trends are also found for changes to the aromatic diamine identity in the ODPA family. When changing from a more bulky fluorinated diamine to a less bulky ether-containing diamine, the aromatic polyimide phase changes in structure significantly due to ring regularity from the planarity and volume of the molecules. The type and length scale of aromatic ordering can be tuned. These factors can lead to dramatic changes in polymer chain mobility, ionic liquid uptake, structure and, ultimately, conductivity.

It should be noted that there are still many other properties that need to be examined in order to fully evaluate these materials for use in fuel cells. One crucial property includes the loss or leakage of ionic liquid from the polymer membranes which has been found to be a concern in other work on ionic liquid-doped polymer systems.[69] Other properties that are also integral for operation in a fuel cell include mechanical strength and gas permeability, especially for hydrogen and oxygen. Future experiments should include the quantitative assessment of these properties as well as fuel cell operation data.

REFERENCES AND NOTES

1 M. J. Park, I. Choi, J. Hong, O. Kim, *J. Appl. Polym. Sci.* **2013**, *129*, 2363–2376.

2 A. F. Baldwin, R. Ma, C. Wang, R. Ramprasad, G. A., Sotzing, *J. Appl. Polym. Sci.* **2013**, *130*, 1276–1280.

3 H. Bourne, G. C. Eastmond, M. Gibas, W. F. Pacynko, J. Paprotny, *J. Membr. Sci.* **2002**, *207*, 17–27.

4 S. Gassara, W. Chinpa, D. Quemener, R. Ben Amar, A. Deratani, *J. Membr. Sci.* **2013**, *436*, 36–46.

5 A. Marcos-Fernández, A. Tena, A. E. Lozano, J. G. de la Campa, J. de Abajo, L. Palacio, P. Prádanos, A. Hernández, *Eur. Polym. J.* **2010**, *46*, 2352–2364.

6 A. Tena, A. E. Lozano, L. Palacio, A. Marcos-Fernández, P. Prádanos, J. de Abajo, A. Hernández, *Int. J. Greenh. Gas Control* **2013**, *12*, 146–154.

7 A. Tena, A. Marcos-Fernández, L. Palacio, P. Cuadrado, P. Pradanos, J. de Abajo, A. E. Lozano, A. Hernandez, *Ind. Eng. Chem. Res.* **2012**, *51*, 3766–3775.

8 A. Tena, A. Marcos-Fernández, L. Palacio, P. Prádanos, A. E. Lozano, J. de Abajo, A. Hernández, *J. Membr. Sci.* **2013**, *434*, 26–34.

9 H. Bai, W. W. Ho, *Polym. Int.* **2011**, *60*, 26–41.

10 M. A. Hickner, H. Ghassemi, Y. S. Kim, B. R. Einsla, J. E. McGrath, *Chem. Rev.* **2004**, *104*, 4587–4612.

11 J. Song, M.-H. Ryou, B. Son, J.-N. Lee, D. J. Lee, Y. M. Lee, J. W. Choi, J.-K. Park, *Electrochim. Acta* **2012**, *85*, 524–530.

12 H. Koerner, R. J. Strong, M. L. Smith, D. H. Wang, L.-S. Tan, K. M. Lee, T. J. White, R. A. Vaia, *Polymer (Guildf).* **2013**, *54*, 391–402.

13 H. Bai, W. S. W. Ho, *J. Membr. Sci.* **2008**, *313*, 75–85.

14 S. Bose, T. Kuila, T. X. H. Nguyen, N. H. Kim, K.-T. Lau, J. H. Lee, *Prog. Polym. Sci.* **2011**, *36*, 813–843.

15 A. Morikawa, F. Miyata, J. Nishimura, *High Perform. Polym.* **2012**, *24*, 783–792.

16 S. Pandiyan, D. Brown, N. F. A. Van Der Vegt, S. Neyertz, *J. Polym. Sci., Part B: Polym. Phys.* **2009**, *47*, 1166–1180.

17 N. Ritter, I. Senkovska, S. Kaskel, J. Weber, *Macromolecules* **2011**, *44*, 2025–2033.

18 A. Shimazu, T. Miyazaki, K. Ikeda, *J. Membr. Sci.* **2000**, *166*, 113–118.

19 J. Wakita, S. Jin, T. J. Shin, M. Ree, S. Ando, *Macromolecules* **2010**, *43*, 1930–1941.

20 Y. Shoji, R. Ishige, T. Higashihara, J. Morikawa, T. Hashimoto, A. Takahara, J. Watanabe, M. Ueda, *Macromolecules* **2013**, *46*, 747–755.

21 Z.-H. Shen, A. J. Jing, S. Jin, H.-B. Wang, F. W. Harris, S. Z. D. Cheng, *Chin. J. Polym. Sci.* **2005**, *23*, 171–187.

22 R. Pan, T. Zhou, A. Zhang, W. Zhao, Y. Gu, *J. Polym. Sci. Part B: Polym. Phys.* **2010**, *48*, 2257–2261.

23 H. Niu, M. Huang, S. Qi, E. Han, G. Tian, X. Wang, D. Wu, *Polymer (Guildf).* **2013**, *54*, 1700–1708.

24 J. T. Muellerleile, B. G. Risch, D. E. Rodrigues, L. Garth, *Techniques* **1993**, *34*, 789–806.

25 S. L. Liu, T. S. Chung, H. Oikawa, A. Yamaguchi, *J. Polym. Sci. Part B: Polym. Phys.* **2000**, *38*, 3018–3031.

26 L. Feng, J. O. Iroh, *Eur. Polym. J.* **2013**, *49*, 1811–1822.

27 V. Bershtein, T. Sukhanova, T. Krizan, M. Keating, A. Grigoriev, V. Egorov, P. Yakushev, N. Peschanskaya, M. Vylegzhanina, A. Bursian, *J. Macromol. Sci. Part B: Phys.* **2005**, *44*, 613–639.

28 V. A. Bershtein, L. M. Egorova, P. N. Yakushev, O. Meszaros, P. Sysel, L. David, A. Kanapitsas, P. Pissis, *J. Macromol. Sci.* **2002**, *41*, 419–450.

29 S. Isoda, H. Shimada, M. Kochi, H. Kambe, *J. Polym. Sci. Polym. Phys. Ed.* **1981**, *19*, 1293–1312.

30 S. P. Ma, T. Takahashi, *Polymer (Guildf).* **1996**, *37*, 5589–5596.

31 B. B. Sauer, B. S.Hsiao, *Polymer (Guildf).* **1995**, *36*, 2553–2558.

32 A. Tena, A. Marcos-Fernández, A. E. Lozano, J. G. de la Campa, J. de Abajo, L. Palacio, P. Prádanos, A. Hernández, *J. Membr. Sci.* **2012**, *387*, 54–65.

33 A. Tena, M. de la Viuda, L. Palacio, P. Prádanos, A. Marcos-Fernández, A. E. Lozano, A. Hernández, *J. Membr. Sci.* **2014**, *453*, 27–35.

34 A. Orzezsko, *J. Appl. Polym. Sci.* **1991**, *42*, 873–875.

35 D. Munoz, E. Maya, J. Deabajo, J. Delacampa, A. Lozano, *J. Membr. Sci.* **2008**, *323*, 53–59.

36 E. M. Maya, D. M. Muñoz, J. G. de la Campa, J. de Abajo, A. E. Lozano, *Desalination* **2006**, *199*, 188–190.

37 H. R. Kricheldorf, G. Schwarz, M. Berghahn, J. de Abajo, J. G. de la Campa, *Macromolecules* **1994**, *27*, 2540–2547.

38 G. C. Eastmond, J. Paprotny, *Polymer (Guildf).* **2002**, *43*, 3455–3468.

39 G. C. Eastmond, M. Gibas, W. F. Pacynko, J. Paprotny, *J. Membr. Sci.* **2002**, *207*, 29–41.

40 G. Costa, G. C. Eastmond, J. P. A. Fairclough, J. Paprotny, A. J. Ryan, P. Stagnaro, *Macromolecules* **2008**, *41*, 1034–1040.

41 K. Okamoto, M. Fujii, S. Okamyo, H. Suzuki, K. Tanaka, H. Kita, *Macromolecules* **1995**, *28*, 6950–6956.

42 K. Okamoto, N. Umeo, S. Okamyo, K. Tanaka, H. Kita, *Chem. Lett.* **1993**, *22*, 225–228.

43 D. M. Tigelaar, A. E. Palker, M. A. B. Meador, W. R. Bennett, *J. Electrochem. Soc.* **2008**, *155*, A768–A774.

44 C. Jung, M. Jikei, M. Kakimoto, *Opt. Soc. Am. B* **1998**, *15*, 471–476.

45 Q. Li, X. Yang, W. Chen, C. Yi, Z. Xu, *Macromol. Symp.* **2008**, *261*, 148–156.

46 P. Liu, *Iran. Polym. J.* **2005**, *14*, 968–972.

47 J. Yang, M. A. Lee, *Macromol. Res.* **2004**, *12*, 263–268.

48 H. Chen, Y. Xiao, T. -S. Chung, *Polymer (Guildf).* **2010**, *51*, 4077–4086.

49 R. M. Huertas, C. M. Doherty, A. J. Hill, A. E. Lozano, J. de Abajo, J. G. de la Campa, E. M. Maya, *J. Membr. Sci.* **2012**, *409-410*, 200–211.

50 E. M. Maya, D. M., Munoz, A. E. Lozano, J. De Abajo, J. G. De La Campa, *J. Polym. Sci. Part A: Polym. Chem.* **2008**, *46*, 8170–8178.

51 C. A. Vincent, *Prog. Solid State Chem.* **1987**, *17*, 145–261.

52 P. V. Wright, *Electrochim. Acta* **1998**, *43*, 1137–1143.

53 Y. N. Lazareva, M. N. Vidyakin, A. Y. Alentiev, M. Y. Yablokova, A. A. Kuznetsov, I. A. Ronova, *Polym. Sci. Ser. A* **2009**, *51*, 1068–1074.

54 B. T. Low, Y. Xiao, T. S. Chung, *Polymer (Guildf).* **2009**, *50*, 3250–3258.

55 Q. Fu, B. P. Livengood, C. C. Shen, F. L. Lin, F. W. Harris, S. Z. D. Cheng, B. S. Hsiao, F. Yeh, *Macromol. Chem. Phys.* **1998**, *199*, 1107–1118.

56 L. Gwee, J. H. Choi, K. I. Winey, Y. A. Elabd, *Polymer (Guildf).* **2010**, *51*, 5516–5524.

57 S. Y. Kim, S. Kim, M. J. Park, *Nat. Commun.* **2010**, *1*, 1–7.

58 P. M. Simone, T. P. Lodge, *ACS Appl. Mater. Interfaces* **2009**, *1*, 2812–20.

59 W. S. Young, W. F. Kuan, T. H. Epps, *J. Polym. Sci. Part B: Polym. Phys.* **2014**, *52*, 1–16.

60 R. O'Hayre, S.-W. Cha, W. Colella, F. B. Prinz, *Fuel Cell Fundam.* **2009**.

61 J. Qiao, N. Yoshimoto, M. Ishikawa, M. Morita, *Electrochim. Acta* **2002**, *47*, 3441–3446.

62 J. P. Curtet, D. Djurado, M. Bee, C. Michot, M. Armand, *Synth. Met.* **1999**, *102*, 1412–1413.

63 D. Djurado, J. P. Curtet, J. F. Legrand, M. Bee, C. Michot, M. Armand, *Synth. Met.* **1997**, *84*, 989–990.

64 D. Djurado, J. Curtet, M. Bee, C. Michot, M. Armand, *Electrochim. Acta* **2007**, *53*, 1497–1502.

65 C. Xue, M. A. B. Meador, L. Zhu, J. J. Ge, S. Z. D. Cheng, S. Putthanarat, R. K. Eby, A. Khalfan, G. D. Bennett, S. G. Greenbaum, *Polymer (Guildf).* **2006**, *47*, 6149–6155.

66 P. P. Huo, J. B. Friler, P. Cebe, *Polymer (Guildf).* **1993**, *34*, 4387–4398.

67 M. Ree, T. L. Nunes, J. S. Lin, *Polymer (Guildf).* **1994**, *35*, 1148–1156.

68 S. Srinivas, G. L. Wilkes, *Polymer (Guildf).* **1998**, *39*, 5839–5851.

69 B. Lin, S. Cheng, L. Qiu, F. Yan, S. Shang, J. Lu, *Chem. Mater.* **2010**, *22*, 1807–1813.